

SPH simulation of boron carbide under shock compression with different failure models

S A Dyachkov^{1,2}, A N Parshikov¹, V V Zhakhovsky¹

¹Dukhov Research Institute of Automatics, ROSATOM, Moscow, 127055, Russia

²Moscow Institute of Physics and Technology, Dolgoprudny, 141700, Russia

E-mail: serj.dyachkov@gmail.com

Abstract. Boron carbide behavior under shock compression is analyzed by comparison of SPH simulations with two sets of plate-impact experiments where the used samples were manufactured using different technology. Various boron carbide failure models are applied to determine the relevant mechanical properties which are responsible for the velocity profiles obtained from VISAR measurements. We show that in order to fit the experimental profiles the strength of the failed state of material should be different in those experiments. This strength is demonstrated to be a unique function of pressure irrespective of the utilized failure models.

1. Introduction

Boron carbide response to high-strain rate shock compression leading to large deformations is of present-day interest. Due to its unique strength properties boron carbide has numerous applications. Nevertheless, under shock loading it is involved into a process of failure [1] what significantly reduces its strength as demonstrated in plate-impact experiments [2].

The comprehensive models for ceramics under shock loading including boron carbide [1, 3] provide all necessary data for simulations of experiments [2]. However, it was found [1] that boron carbide samples behave as different materials in different sets of experiments. For instance, the data [4] cannot be reproduced with provided model parameters and the previous model [5] should be used. The reason for that may be due to different manufacturing technology for boron carbide samples.

In this research we provide a new understanding of manufacturing dependent boron carbide characteristics which define its behavior under shock compression. The analysis is based on the three dimensional SPH simulations of wave profiles in accordance with two different sets of plate-impact experiments [2, 4]. We use the strength model for boron carbide failure based on Johnson and Holmquist models [1, 5] and a more simple approach with yield strength temperature dependence.

2. Equation of state for boron carbide under hydrostatic stress

Complex structure of boron carbide causes difficulties in its equation of state definition. In the range of parameters of our interest there is a question about structural phase transition leading to discontinuous volume change. Experimental observation of boron carbide under hydrostatic stress in diamond anvil cells does not demonstrate such kind of behavior [6]. That fact was also



proved by DFT calculations [7]. However, at non-hydrostatic stress the question about phase transition is still arguable, but relevant information about it is unavailable.

In our simulations we use a Mie-Gruneisen form for the equation of state:

$$P = P_0 + \Gamma \rho (e - e_0), \quad (1)$$

$$P_0 = \frac{\rho_0 c_0^2}{n} (\delta^n - 1), \quad (2)$$

$$e_0 = \frac{c_0^2}{n} \left(\frac{\delta^{n-1} - 1}{n-1} + \frac{1}{\delta} - 1 \right), \quad (3)$$

$$\delta = \frac{\rho}{\rho_0}, \quad (4)$$

$$\Gamma = 1.625 \left(\frac{\rho_0}{\rho} - 1 \right) + 0.54, \quad (5)$$

with parameters fitted according to hydrostatic compression of boron carbide in quantum molecular dynamics simulation [7]. The parameters ρ_0 , c_0 , n are given in the Table 1. In contrast to [1] we do not use any kind of phase transition in this equation of state.

Table 1. B₄C properties.

Material characteristic	Value
Initial density ρ_0 , kg/m ³	2550
Sound velocity c_0 , km/s	10
EoS exponent n	3
Poisson ratio ν	0.162
Bulk modulus K , GPa	255
Shear modulus G , GPa	216
Hugoniot Elastic Limit (HEL), GPa	18.2
HEL strength σ_{HEL} , GPa	14.0
HEL pressure P_{HEL} , GPa	8.8
HEL volumetric strain μ	0.035
Intact strength constant σ_i^0 , GPa	6.7
Intact strength constant σ_i^{\max} , GPa	14.3
Intact strength constant P_i , GPa	2.3
Failure strength constant σ_f^0 , GPa	1.0/5.0
Failure strength constant σ_f^{\max} , GPa	2.0/8.5
Failure strength constant P_f , GPa	2.0/5.0
Hydrostatic tensile strength T , GPa	0.27
Strain rate constant C	0.01
Bulking factor β	1.0

3. Boron carbide failure models

Johnson and Holmquist [1, 5] consider the strength models for boron carbide failure under compression. The idea is that failure begins as soon as von Mises equivalent stress σ_e reaches intact strength limit σ_i . Numerous plate impact experiments with ceramics demonstrate hydrostatic pressure dependency for the intact strength. Below the curve $\sigma_i(P)$ the damage

zone is located. Boron carbide has significantly lower strength limit $\sigma_f(P)$ for the failed state, and during failure process the damaged material strength limit σ_d reduces from σ_i to σ_f :

$$\sigma_d = \sigma_i - D(\sigma_i - \sigma_f) \quad (6)$$

where D is the damage factor which indicates an amount of accumulated damage starting from 0 (intact) to 1 (failed).

Recent JHB model [1, 3] uses similar form for the intact ($\lambda = i$) and failed ($\lambda = f$) stresses:

$$\begin{cases} \sigma_\lambda = \sigma_\lambda^0 + (\sigma_\lambda^{\max} - \sigma_\lambda^0)\{1.0 - \exp[-\alpha_\lambda(P - P_\lambda)]\}, & P > P_\lambda, \\ \sigma_\lambda = \sigma_\lambda^0 P / (P_\lambda + T), & P < P_\lambda, \end{cases} \quad (7)$$

$$\alpha_\lambda = \sigma_\lambda^0 / [(\sigma_\lambda^{\max} - \sigma_\lambda^0)(P_\lambda + T)] \quad (8)$$

with a difference that hydrostatic tensile strength $T = 0$ for the failed state. The constants σ_λ^0 , σ_λ^{\max} , P_λ are defined in accordance with experimental data. It should be noted, that strain rate dependency is also included to the intact and failed curves as follows:

$$\sigma_\lambda(\dot{\epsilon}^*) = \sigma_\lambda(1.0 + C \ln \dot{\epsilon}^*) \quad (9)$$

where $\dot{\epsilon}^* = \dot{\epsilon} / \dot{\epsilon}_0$ – dimensionless equivalent strain rate for $\dot{\epsilon}_0 = 1.0 \text{ s}^{-1}$, C – constant. In three dimensions equivalent strain can be found as:

$$\dot{\epsilon} = \sqrt{\frac{2}{9} \left[(\dot{\epsilon}_{xx} - \dot{\epsilon}_{yy})^2 + (\dot{\epsilon}_{yy} - \dot{\epsilon}_{zz})^2 + (\dot{\epsilon}_{xx} - \dot{\epsilon}_{zz})^2 + \frac{3}{2}(\dot{\gamma}_{xy}^2 + \dot{\gamma}_{yz}^2 + \dot{\gamma}_{xz}^2) \right]}. \quad (10)$$

If process of failure take place, damage D is accumulated according to the kinetic equation:

$$\frac{dD}{dt} = \frac{\dot{\epsilon}_p}{\epsilon_p^f}, \quad (11)$$

where $\dot{\epsilon}_p$ – plastic strain rate, ϵ_p^f – total plastic strain to failure. Plastic strain for a cycle of integration $\Delta\epsilon_p$ can be estimated [8]

$$\dot{\epsilon}_p \Delta t = \Delta\epsilon_p = \frac{\hat{\sigma}_e^t - \sigma_e^t}{3G}, \quad (12)$$

where $\hat{\sigma}_e^t$ is equivalent stress calculated at the time step t , but not corrected:

$$\hat{\sigma}_e = \sqrt{\frac{1}{2} \left[(\hat{S}_{xx} - \hat{S}_{yy})^2 + (\hat{S}_{yy} - \hat{S}_{zz})^2 + (\hat{S}_{xx} - \hat{S}_{zz})^2 + 6(\hat{S}_{xy}^2 + \hat{S}_{xz}^2 + \hat{S}_{yz}^2) \right]}. \quad (13)$$

The resulting stress limit for the damaged material σ_d may be found as (6) using current damage factor D^t . Equivalent stress σ_e must be below σ_d , so if necessary ($\hat{\sigma}_e > \sigma_d$), we apply the correction to stresses:

$$S_{\alpha\beta} = \frac{\sigma_d}{\hat{\sigma}_e} \hat{S}_{\alpha\beta}, \quad \sigma_e = \sigma_d. \quad (14)$$

Using corrected equivalent stress σ_e one can find the plastic strain increment $\Delta\epsilon_p$.

In the original Johnson-Holmquist model [1, 5] the amount of plastic strain to failure ϵ_p^f is independent of other model parameters what provides additional degree of freedom. But for instant failure (D changes from 0 to 1 in one step) one can notice that plastic strain to failure is

$$\Delta\epsilon_p = \frac{\sigma_i - \sigma_f}{3G} = \epsilon_p^f. \quad (15)$$

For the model to be consistent this expression should be used throughout whole fragmentation process. Thus one can define damage at the next step $t + \Delta t$ as follows:

$$D^{t+\Delta t} = D^t + \frac{\hat{\sigma}_e^t - \sigma_e^t}{\sigma_i - \sigma_f}. \quad (16)$$

Additional pressure ΔP is then added due to bulking of damaged material [5]

$$P_{\text{total}} = P_{\text{EoS}} + \Delta P. \quad (17)$$

It can be estimated, for example, by evaluating elastic energy loss ΔU during a cycle of integration:

$$\Delta U = \frac{(\sigma_e^2)_t}{6G} - \frac{(\sigma_e^2)_{t+\Delta t}}{6G}, \quad (18)$$

and then expressed as:

$$\Delta P^{t+\Delta t} = -K\mu + \sqrt{(K\mu + \Delta P^t) + 2\beta K \Delta U}, \quad (19)$$

where K – bulk modulus, $\mu = \rho/\rho_0 - 1$, β – bulking factor. Further we will refer to this model as JH-based model.

The damage parameter D can be also evaluated as a function of state without kinetic equation. For example, one can add yield strength Y dependency of specific thermal energy e_T what similarly to previous model reduces yield strength from intact Y_i to failed Y_f . For the damage parameter D the following equation is used:

$$D = e_T/e_D, \quad (20)$$

where e_D is the thermal energy of totally failed material. Then the yield strength for damaged material Y_d is defined similar to (6):

$$Y_d = Y_i - D(Y_i - Y_f). \quad (21)$$

Yield strength for the failed material can be taken in the form (8). Further we will refer to this model as Y-based model.

4. Simulation of plate impact experiments

Validation of the presented boron carbide model is performed by comparison with Grady et al. [4] and Vogler et al. [2] plate impact experiments. Simulation setup is shown in the figure 1: an impactor with backer foam hits a boron carbide target producing shock wave which propagates to a lithium fluoride window. Experimental measurements of velocity profiles at the B_4C /LiF interface provided by a VISAR. In SPH simulations the particles at this interface are tracked and their velocities are averaged for a profile.

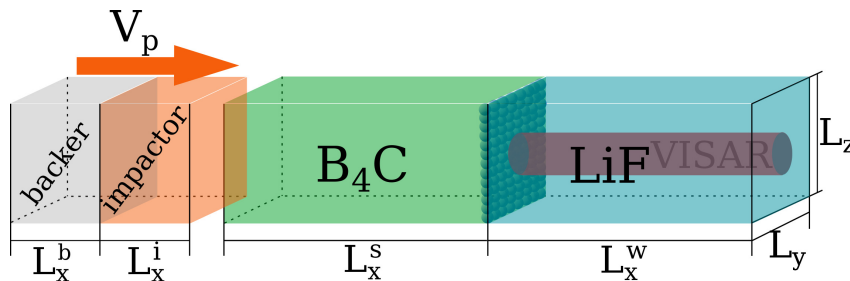


Figure 1. Simulation setup for boron carbide plate impact experiments. Impactor with backer material obtain initial velocity V_p in direction to B_4C target. After collision the shock wave propagates to the interface between boron carbide and lithium fluoride where the velocity of B_4C surface is measured as an average of SPH particle velocities.

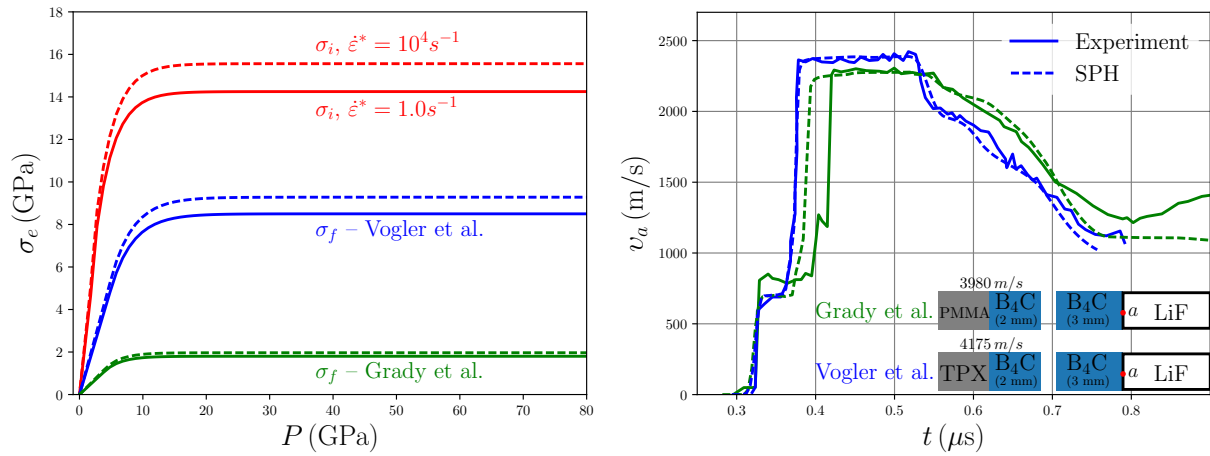


Figure 2. Influence of boron carbide strength at the failed state on wave profiles. Both experiments BC10 and BC-X have similar initial setup, but profiles are rather distinct. SPH simulation with JH-based model and different dependency $\sigma_f(P)$ is shown to be in agreement with each of both experiments.

Each simulated sample has sizes $L_y \times L_z = 0.1 \times 0.1$ mm, and L_x in accordance with specific experiment. Periodic boundary conditions are applied for y and z axes. SPH particles are packed in a dense liquid-like mesh in order to avoid regular grid packing effects. For y and z axes there are an average of 17.5 particles and several thousands for x axis depending on initial data. The SPH kernel Wendland-C² [9] and the appropriate Riemann solver [10] are used for our contact modification of SPH [11].

The equation of state for boron carbide provides new bulk modulus $K = \rho_0 c_0^2 = 255$ GPa, so that one have to adjust HEL and other strength properties given in [1]. Using the same HEL volumetric strain $\mu = 0.035$ and Poisson ratio we get new values for G and σ_i (see Table 1). For the Y-based model we use $Y_i = 24.3$ GPa, $e_D = 1.547 \times 10^5$ J/kg, and the same parameters for material at the failed state: $Y_f^0 = \sigma_f^0$, $Y_f^{\max} = \sigma_f^{\max}$.

As a result of our simulations we noticed that velocity profiles in different sets of experiments are very sensitive to failed material strength σ_f in both models. Figure 2 demonstrates that two experimental profiles with similar initial setup (BC10 from Grady et al. and BC-X from Vogler et al.) should be simulated with a different strength at the failed state. The reduction of σ_f leads both to elongation of the elastic precursor and smaller amplitude of elastic release what corresponds experimental data. So that in the Table 1 there are two sets of values for $\sigma_f^0, \sigma_f^{\max}, P_f$: first is found for Grady et al. experiments, second is for Vogler et al.

Our simulations of other experiments also demonstrate good agreement (Figure 3). Different boron carbide failure kinetics implemented in JH-based and Y-based models does not appear to affect velocity profile as much as different failed strength σ_f . This property seems to be dependent on boron carbide production technology and can be adjusted by fitting specific velocity profiles.

5. Conclusion

In this research we considered two boron carbide failure models: Johnson-Holmquist based strength model with kinetic equation for damage accumulation and non-kinetic model with thermal dependency for yield strength. Using both models with the same equation of state we performed simulations via contact SPH method for three dimensional samples with periodical boundary conditions and achieved good agreement with the experiments [2, 4]. As it was

mentioned earlier [1], different manufactured flavors of boron carbide provide different velocity profiles for plate-impact experiments. We found that the main characteristic that guides boron carbide behavior under shock compression is material strength σ_f at the failed state. It was demonstrated that the strength σ_f is a unique function of material and applied pressure irrespective of the utilized failure models, and it can be adjusted for a specific flavor of boron carbide.

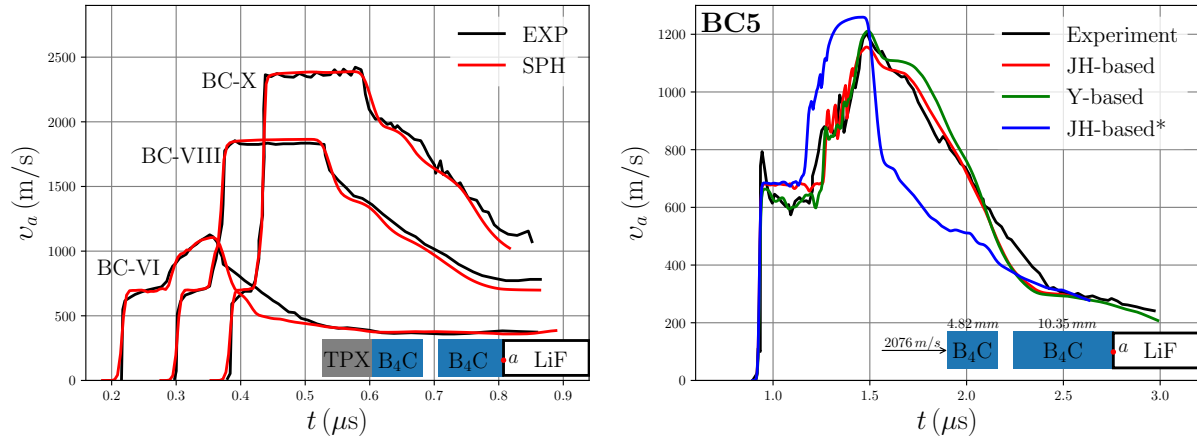


Figure 3. Experimental and simulated by SPH boron carbide wave profiles. On the left three experiments are simulated using JH-based model with σ_f fitted to Vogler et al. data. On the right experiment BC5 by Grady et al. is simulated using two different models: JH-based and Y-based which are in good agreement. However, using σ_f based on Vogler et al. data* the resulting profile become rather distinct.

Acknowledgements

This work is supported by the Russian Science Foundation grant 14-19-01599.

References

- [1] Holmquist T J and Johnson G R 2006 *Journal of Applied Physics* **100** 093525
- [2] Vogler T, Reinhart W and LC C 2004 *Journal of Applied Physics* **95** 4173–4183
- [3] Johnson G R, Holmquist T J and Beissel S R 2003 *Journal of Applied Physics* **94** 1639–1646
- [4] Grady D and Moody R 1996 Shock compression profiles in ceramics Tech. rep. Sandia Report SAND96-0551
- [5] Johnson G R and Holmquist T J 1999 *Journal of Applied Physics* **85** 8060
- [6] Dera P, Manghnani M H, Hushur A, Hu Y and Tkachev S 2014 *Journal of Solid State Chemistry* **215** 85–93
- [7] Korotaev P, Pokatashkin P and Yanilkin A 2016 *Modelling and Simulation in Materials Science and Engineering* **24** 015004
- [8] Wilkins M L 1999 *Computer Simulation of Dynamic Phenomena* (Springer-Verlag Berlin Heidelberg)
- [9] Wendland H 1995 *Advances in computational Mathematics* **4** 389–396
- [10] Dukowicz J K 1985 *Journal of Computational Physics* **61** 119–137
- [11] Parshikov A N and Medin S A 2002 *Journal of computational physics* **180** 358–382